ADVANCES IN ATMOSPHERIC SCIENCES, VOL. 31, MAY 2014, 604–610

Aircraft Observations of Liquid and Ice in Midlatitude Mixed-Phase Clouds

ZHAO Zhen* and LEI Hengchi

Key Laboratory of Cloud-Precipitation Physics and Severe Storms, Institute of Atmospheric Physics, Chinese Academy of Sciences, Beijing 100029

(Received 5 May 2013; revised 10 July 2013; accepted 12 August 2013)

ABSTRACT

This paper reports airborne measurements of midlatitude altostratus clouds observed over Zhengzhou, Henan Province, China on 3 March 2007. The case demonstrates mixed-phase conditions at altitudes from 3200 to 4600 m (0°C to −7.6°C), with liquid water content ranging from 0.01 to 0.09 g m^{-3}. In the observed mixed-phase cloud, liquid water content exhibited a bimodal distribution, whereas the maximum ice particle concentration was located in the middle part of the cloud. The liquid and ice particle data showed significant horizontal variability on the scale of a few hundred meters. The cloud droplet concentration varied greatly over the horizontal sampling area. There was an inverse relationship between the cloud droplet concentration and ice particle concentration.

A gamma distribution provided the best description of the cloud droplet spectra. The liquid droplet distributions were found to increase in both size and concentration with altitude. It was inferred from the profile of the spectra parameters that the cloud droplet sizes tend to form a quasi-monodisperse distribution. Ice particle spectra in the cloud were fitted well by an exponential distribution. Finally, a remarkable power law relationship was found between the slope (λ) and intercept (N_0) parameters of the exponential size distribution.

Key words: cloud structure, liquid water content, droplet spectra, particle measuring systems

Citation: Zhao, Z., and H. C. Lei, 2014: Aircraft observations of liquid and ice in midlatitude mixed-phase clouds. *Adv. Atmos. Sci.*, **31**(3), 604–610, doi: 10.1007/s00376-013-3083-2.

1. Introduction

In the temperature range from 0°C to −40°C, the coexistence of liquid water droplets and ice particles in single-layered clouds are usually called "mixed-phase" clouds. The microphysical properties of mixed-phase clouds are relatively unknown and need further observational study. Cober et al. (2001b) observed 26% and 46% of mixed-phase conditions during the first and third "Canadian freezing drizzle experiments", respectively. In addition, recent observational results show that 40%–60% of clouds are mixed phase in various regions, and even globally (Mazin, 2006; Shupe et al., 2006; Zhang et al., 2010).

It is important to understand the physics of mixed-phase conditions for climate (Fowler and Randall, 1996; Rotstayn, 1997; Choi et al., 2010), radiative transfer (Sun and Shine, 1994), and remote sensing research (Young et al., 2000; Zhong et al., 2011). The mixed-phase cloud is also closely related to precipitation formation, cloud electrification (Williams et al., 1991), as well as weather modification and aircraft icing.

There are many demands on accurate measurements of cloud liquid water content (LWC) and droplet spectra for applied problems in mixed-phase clouds. For example, the cloud LWC and droplet spectrum median volume diameter can represent aircraft icing environments (Cober et al., 1996; Cober et al., 2001a). The vertical distribution of liquid water and ice has a strong influence on modeling radiative transfer in mixed-phase clouds (Niu et al., 2008). Understanding cloud ice crystal evolution is of great importance for cloud physics development. Previous studies (Lo and Passarelli, 1982; Gordon and Martwitz, 1986; Field, 1999; Wolde and Vali, 2002) have shown that the evolution of ice particles in mixed-phase clouds takes place first by depositional growth in the upper level, and is then followed by aggregation growth of larger ice particles. Evidence for this sequence comes from aircraft measurements of ice particle shapes and spectra.

However, in the midlatitude region, observations of mixed-phase clouds are relatively sparse. Hobbs and Rangno (1985) observed maximum liquid water and small amounts of ice particles at the altocumulus cloud top. Heymsfield et al. (1991) found altocumulus cloud has a thin, highly supercooled liquid water layer at cloud top. Hogan et al. (2003) investigated two case clouds consisting of a supercooled liquid water layer above or embedded within ice clouds. Carey et al. (2008) reported peak liquid water content occurs at or near the cloud top, while peak ice water content occurs in the lower half of the cloud or in virga. Noh et al. (2013)

* Corresponding author: ZHAO Zhen
Email: zhaozhen@mail.iap.ac.cn

studied the vertical profiles of various mixed-phase clouds using *in situ* aircraft observations and found that shallower clouds have higher liquid water, while deeper clouds contain more ice.

The present paper reports results from an *in situ* aircraft study of microphysical parameters collected in mixed-phase altostratus clouds. The purpose of the study is to help expand knowledge of the microphysics of liquid water and ice in midlatitude mixed-phase clouds through analysis of vertical profiles. The structure of the paper is as follows. In section 2 the observational instrumentation is discussed. In section 3 the experimental observations are outlined. In section 4 the results of the observations are presented. And finally, conclusions are drawn in section 5.

2. Instrumentation

The measurements reported in this paper were collected aboard the Henan Province Weather Modification Bureau Y-12E research aircraft. This airborne instrument provides measurements of temperature, dewpoint temperature, pressure, and cloud microphysical variables. The aircraft position and altitude were determined by global positioning system (GPS) data.

The cloud microphysical measurements probes, made with Particle Measuring Systems (PMS), include a forward scattering spectrometer probe (FSSP), a two-dimensional cloud (2D-C) probe, and a King liquid water probe (KLWP). It is necessary to discuss the strengths and limitations of each instrument because of the central importance of microphysical measurements to the present study.

The FSSP counts particles in the diameter range 2–47 μm with a 3-μm bin interval by measuring the forward-scattered light from a laser as a particle passes through a laser beam. The FSSP sources of error, as described by Baumgardner (1983) and Dye and Baumgardner (1984), cause limitations to the accuracy of discriminating between liquid droplets and ice particles. Gardiner and Hallett (1985) pointed out that the FSSP droplet spectra may be spurious in the presence of ice particles in mixed-phase clouds. Therefore, large errors are raised for the FSSP-measured LWC in mixed-phase clouds as LWC is proportional to the third power of the diameter. The FSSP measurements may be contaminated by small ice particles, but as Lawson et al. (2001) demonstrated, most ice particles grow rapidly to greater than 25 μm in less than one minute in mixed-phase clouds due to high supersaturation with respect to ice. This gives us some confidence that the FSSP measured almost all of the liquid water droplets in mixed-phase clouds.

The 2D-C probe measures particles in the diameter range 25–800 μm with a 50-μm bin interval, and a detailed description of the process is available in the literature (Knollenberg, 1970). The 2D-C probe is now known to have significant counting and sizing errors that are documented in prior work. Korolev et al. (1991) and Strapp et al. (2001) reported particles being overestimated due to being out-of-focus. Baumgardner and Korolev (1997) and Strapp et al. (2001) described underestimation of smaller particles due to the non-zero response time of the sensing photodiodes. Korolev et al. (1998) showed that the discrete manner of particle image registration leads to losses of particles. To alleviate the poor sampling of low ice number concentration due to the limited 2D-C sample volume, we averaged the 2D-C measurements over 10 s. Drops smaller than or equal to 125 μm in diameter detected in the first two channels of the 2D-C instrument were discarded because of the significant sizing errors that occur in these channels (Korolev et al., 1991, 1998).

The KLWP is a hot wire sensor based on the description of King et al. (1978). Biter et al. (1987) pointed out that as droplet median volume diameters (MVDs) become greater than 40 μm, the response to this device gradually diminishes, while substantial correction is required for MVDs of greater than 100 μm. This problem had little effect on our measurements because of the lack of large cloud droplets. Another error factor is the contamination when there are large numbers of ice particles. Cober et al. (2001b) found the KLWP responds to between 5% and 30% of ice water content, with an average response of approximately 20%. The error increases to about 40% when the airspeed reaches 200 m s^{-1} and the cloud contains high concentrations of small ice particles. This suggested to us a maximum LWC error in the order of 20% and approximately 15% given the aircraft airspeeds of 60 m s^{-1} for the Y-12E on 3 March 2007.

3. Observations

The aircraft data were obtained from flights near Zhengzhou in southeast Henan Province in altostratus clouds (As) associated with a midlatitude upper-level trough (frontal system) on 3 March 2007. Infrared cloud images from the Multifunctional Transport Satellite (MTSAT) at 2-h intervals are presented in Fig. 1. By 0430 UTC the cloud band appears to be well developed around the sampling time and covers Henan Province almost entirely. The final 0630 UTC TBB image shows the cloud band weakened and moved toward the northeast.

The flight pattern employed in this case is shown in Fig. 2. A ladder-like route included repeated ascending (or descending) and level segments. Air Traffic Control (ATC) restrictions prevented access to cloud top altitudes, and so clouds were sampled over longer duration level legs of approximately 32 minutes to obtain horizontal samples of mixed-phase clouds. This period of level flight provided optimal estimation of the temporal and spatial variation of the liquid water and ice patterns in the clouds.

The data from flight were averaged in sequential 10-s intervals, corresponding to a mean horizontal length scale of 0.6 km. The 10-s averaging scale was chosen to offer sufficient PMS measurements for statistical significance. The spectra were calculated from the entire FSSP channel and from the 2D-C probe >125-μm channel to the last channel.

The droplet size distributions (DSD) fit the gamma distri-

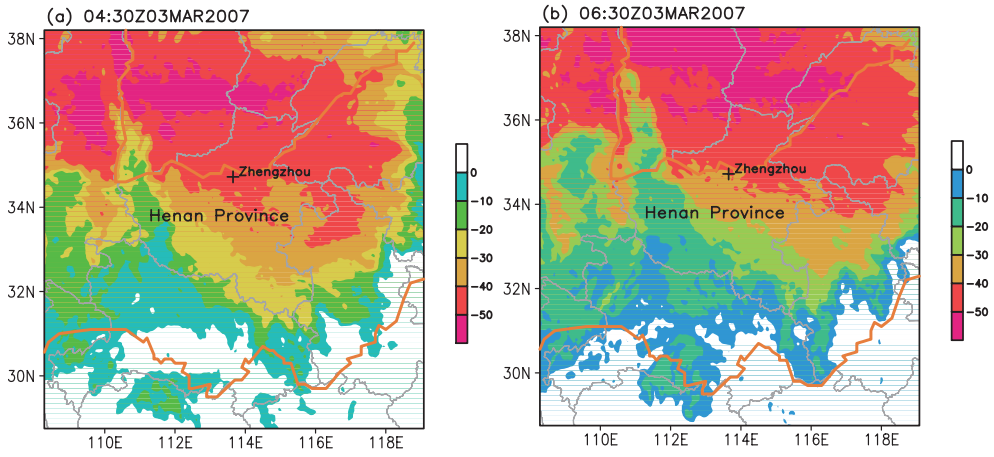

Fig. 1. MTSAT IR blackbody brightness temperature (TBB) distribution (°C) at 2-h intervals from (a) 0430 to (b) 0630 UTC 3 March 2007.

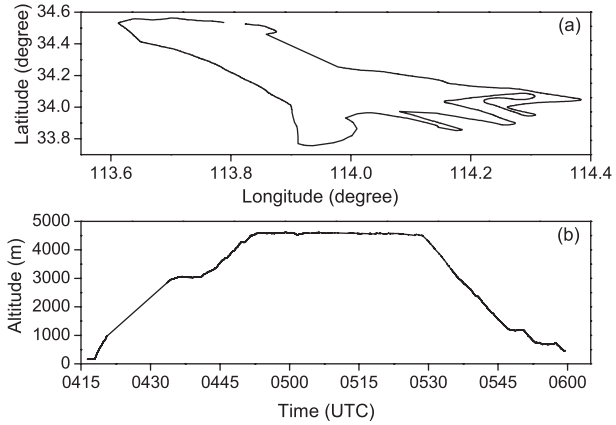

Fig. 2. (a) Horizontal projection of the aircraft flight track and (b) time series of aircraft altitude on 3 March 2007.

bution by Ulbrich (1983),

$$n(D) = N_0 D^{\alpha} e^{-\lambda D}, \qquad (1)$$

where n is particle number concentration per unit size interval, N_0 is the intercept parameter, λ is the slope parameter and α is the shape parameter. Here, D is the actual particle size measured by the FSSP and 2D-C probe. It should be pointed out that 2D-C spectra fit with the exponential distribution (gamma case for $\alpha = 0$).

4. Results

4.1. *Liquid water content and concentration*

Vertical profiles of key parameters from the aircraft measurements are shown in Fig. 3. In regions that were above the melting level, there was a supercooled cloud water layer where the mean LWC value was 0.05 g m^{-3} and the maximum value was 0.09 g m^{-3}, occurring near −4.8°C. The LWC shows a bimodal distribution: one below the cloud top and one near the melting level. A relatively large region of concentrated LWC was observed at temperatures below −4°C. Regions containing substantial cloud droplets were located near the cloud melting level, with the cloud droplet concentration reaching 124 cm^{-3}. Below −2°C, the cloud droplet concentration decreased sharply to within the order of 10 cm^{-3} and was almost constant with increasing altitude. The ice particle concentration measured by 2D-C probe ranged from about 20 to 151 L^{-1}, with a mean of 71 L^{-1}. The maximum ice particle concentration was located in the middle layer at a temperature of −4.8°C, where needle particles and their aggregates were observed in the 2D-C images.

Figures 3a and b show that when cloud droplet concentration decreased, LWC decreased as well. Since LWC is proportional to the third power of the cloud droplet diameter, we conclude that the decrease in LWC showed cloud droplets with small diameters. At the upper level, the variation in LWC was larger than the cloud droplet concentrations, which suggest the diameter of cloud droplets varied a lot.

The time series of LWC, cloud droplet concentration and ice particle concentration during the level-leg measurement period are shown in Fig. 4. It can be seen that there was great variability between the LWC and concentration values of cloud droplets and ice particles, which demonstrates inhomogeneity of As clouds on many scales.

Figure 4 illustrates that when LWC increased, in contrast the cloud droplet concentration decreased. The increase in LWC may have been because of large cloud droplets. It can be seen that when there was an increase in LWC and cloud droplet concentration there was a decrease in ice particle concentration. This suggests that ice particles grow basically by a depositional process at the expense of supercooled water droplets. The presence of some liquid water droplets in larger than 24 μm in diameter (data not shown) and the temperature of this height suggest a potential rime-splintering mechanism for secondary ice crystal production (Hallett and Mossop, 1974).

The general findings of previous observational studies of mixed-phase clouds, as introduced in section 1, are now compared to our measurements. Liquid water content measured by Heymsfield et al. (1991) in the second case was in the

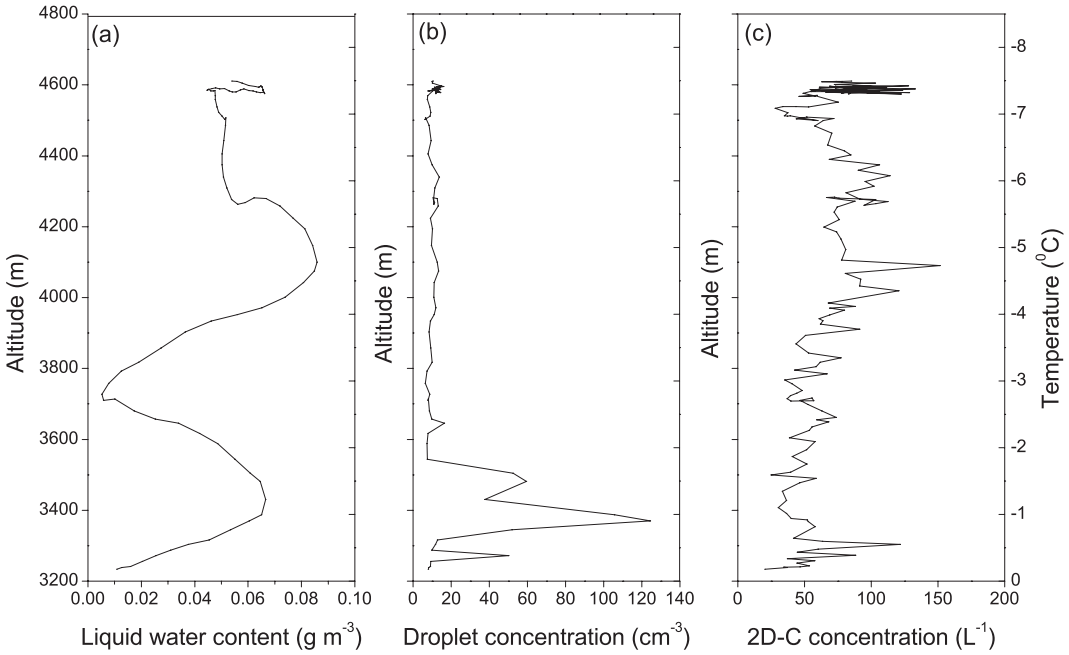

Fig. 3. Vertical profiles of (a) LWC measured by the KLWP, (b) cloud droplet concentration measured by the FSSP, and (c) particle concentration measured by the 2-DC probe during the ascent on 3 March 2007.

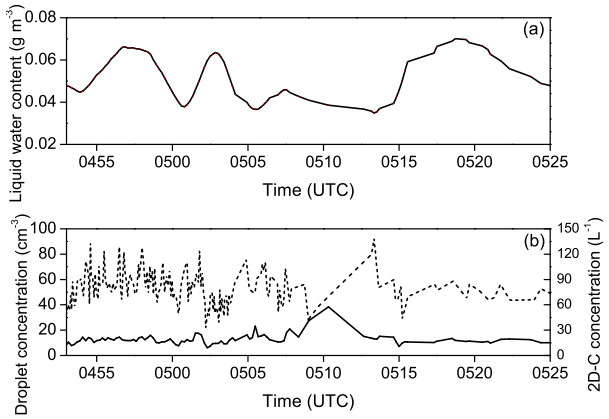

Fig. 4. (a) LWC measured by the KLWP, and (b) cloud droplet concentration measured by the FSSP probe and particle number concentrations measured by the 2-DC probe (dashed line) across the horizontal flight on 3 March 2007.

range 0.04–0.12 g m^{-3}, which is consistent with our observed range. Pinto (1998) found that the LWC of Arctic mixed-phase boundary layer clouds generally increased with altitude, and the maximum value was below the cloud top. This agrees to a certain extent with our measurements. In our observations, LWC had higher values below the cloud top, similar to the results published by Carey et al. (2008).

In China, measurements of cloud microphysical properties with airborne PMS are generally made in the northern parts of the country form spring to autumn, and the results have been reported in several papers. As summarized in Zhang et al. (2011), the maximum supercooled LWC of stratiform clouds in the northern part of China ranges from 0.17 to 0.49 g m^{-3}. Zhang et al. (2011) took 23 aircraft measurements of stratiform clouds over Shandong Province in autumn from 1989 to 2008. The mean supercooled LWC varied from a minimum of 0.0024 g m^{-3} to a maximum of 0.093 g m^{-3}, which was larger than in our study. Fan et al. (2010) examined aircraft-measuerd stratocumulus clouds during August to September in 2004 over Beijing and its surrounding areas. The peak value of supercooled LWC was 0.26 g m^{-3}, which was apparently greater than our observation. These results suggest that there were significant differences between the cloud microphysical properties and formation mechanisms.

4.2. *Cloud droplet and ice particle spectra*

The liquid droplet spectra measured at various altitudes in the mixed-phase cloud by FSSP are shown in Fig. 5. The

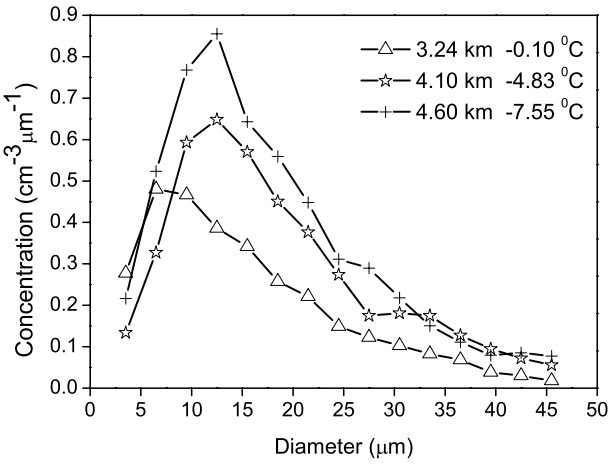

Fig. 5. Liquid droplet spectra at various altitudes during the ascent on 3 March 2007.

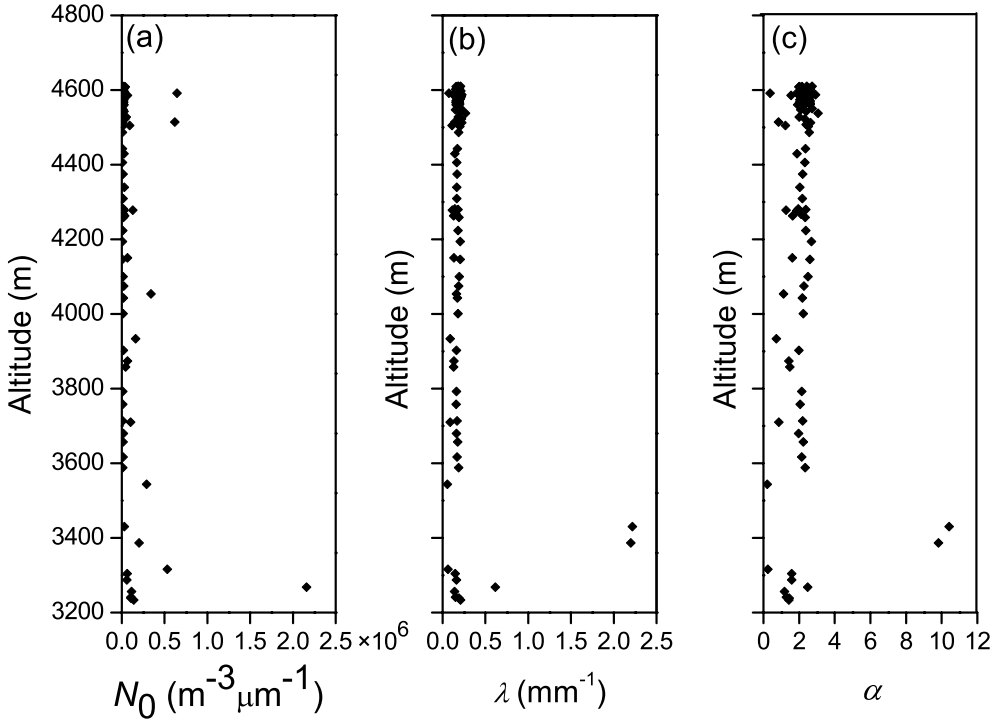

Fig. 6. Vertical profiles of (a) intercept parameter (N_0), (b) the slope parameter (λ), and (c) the shape parameter (α) for the gamma distribution fits to cloud droplet size spectra during the flight on 3 March 2007.

liquid droplet spectra exhibit a feature that both droplet size and concentration increase with altitude through the cloud. This result is consistent with LWC increasing with altitude, as reported in section 4.1.

Gamma distribution functions defined by Eq. (1) were fitted to the observed size spectra for liquid water droplets. The distributions fitted the gamma function with a mean coefficient of determination of $R^2 = 0.96$. Between -0.1°C and -7.6°C (3.2–4.6 km), R^2 values varied from 0.69 to 0.99. The vertical profile of parameters N_0, λ and α calculated from Eq. (1) are shown in Figs. 6a, b and c. The mean N_0, λ and α values were 0.05 cm^{-3} μm^{-1}, 0.20 mm^{-1} and 2.26, respectively. As can be seen from the figures, the general trend is for N_0, λ and α to remain steady with altitude, with a maximum measured value closer to the altitude of 3.4 km just above the melting level. A sudden increase in the spectra parameters λ and α took place at 3.4 km, as shown in Fig. 6. A possible explanation for this λ and α jump is that it resulted from a sudden decrease in the mean diameter of cloud droplets. Given the measured spectra variation is small at various altitudes, the droplet spectra exhibit almost monodisperse distributions.

For the ice particle spectra, exponential functions defined by Eq. (1) for $\alpha = 0$ were fitted to the observed size spectra with a mean coefficient of determination of $R^2 = 0.89$. Figures 7a and b show the vertical profiles of N_0 and λ. The mean N_0 and λ values were 2161.99 m^{-3} μm^{-1} and 8.96 mm^{-1}, respectively. It can be seen that the general trend is for N_0 and λ to increase with altitude, with a maximum measured value closer to the altitude of 4.5 km. Compared to the changes of cloud droplet spectra parameters with altitude, changes in ice particle spectra parameters of N_0 and λ are seen to correlate more strongly with altitude.

Table 1 shows the values of the spectra parameters at various altitudes during the ascent. The values of the λ parameter show that the slope of the 2D-C fitted spectra is approximately 40 times greater than the FSSP fitted spectra, indicating a much faster reduction of the concentration compared to the diameter in the ice particle distribution than in the cloud droplet distribution.

For ice particle spectra, the slope (λ) was plotted against the intercept (N_0) for both the ascent and descent flights, as shown in Fig. 7c. It can be seen that there is strong correlation between λ and N_0 and that the relationship between these two parameters can be expressed by a power law.

5. Conclusions

The present paper describes airborne microphysical measurements that were carried out inside a midlatitude mixed-phase altostratus cloud formed by a frontal system that occurred over Zhengzhou in Henan Province on 3 March 2007.

Mixed-phase condition clouds were sampled from altitudes of 3200 to 4600 m, with temperatures ranging from 0°C to a low of -7.6°C. The maximum liquid water content was 0.09 g m^{-3}, with a mean value in the order of 0.05 g m^{-3}. We observed a bimodal distribution of LWC, whereas the ice particle concentration was at a maximum in

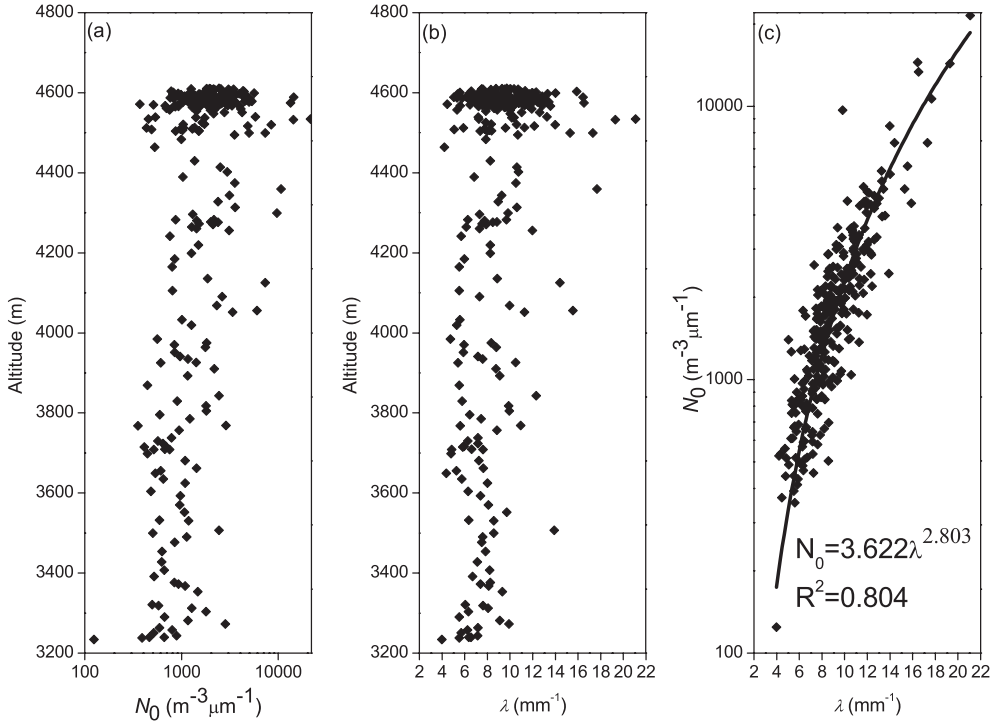

Fig. 7. Vertical profiles of (a) the intercept parameter (N_0) and (b) the slope parameter (λ) for the exponential fits to ice crystal size spectra, and (c) a scatter plot of λ vs. N_0 during the flight on 3 March 2007.

Table 1. Temperature (T), altitude (H), intercept (N_0), slope (λ) and shape parameter (α) parameters for the gamma fit for the FSSP and intercept (N_0) and slope (λ) parameters for the exponential fit for the 2D-C at various altitudes during the ascent on 3 March 2007.

		FSSP			2D-C	
T(°C)	H(km)	N_0(m^{-3} μm^{-1})	λ(mm^{-1})	α	N_0(m^{-3} μm^{-1})	λ(mm^{-1})
−0.10	3.24	0.11×10^6	0.15	1.28	660	6.56
−4.83	4.10	0.01×10^6	0.20	2.50	806	5.51
−7.55	4.60	0.03×10^6	0.19	2.25	1519	7.30

the middle parts of the cloud. Significant horizontal variability was observed in the LWC and concentrations of both cloud droplets and ice particles, corresponding to inhomogeneity in the sampling zone.

The results showed the spectra of cloud droplets and ice particles with diameters under 800 μm. The gamma distribution fitted the cloud droplets reasonably well. From the profile of the spectra parameters, cloud droplet spectra showed a tendency toward a quasi-monodisperse distribution. Cloud droplet sizes and concentrations both increased with increasing altitude in the clouds. It was found that ice particle spectra could be described well by an exponential distribution in the datasets and a power law expression described the relationship between the slope (λ) and intercept (N_0) parameters.

The present reported *in situ* aircraft observation study helps to illustrate the range of variability in hydrometeor microphysical properties such as concentration and spectral parameters. In addition, further *in situ* observations of mixed-phase clouds and new probes, such as the cloud particle imager (CPI), are required to understand and combine the dynamical and microphysical mechanisms of ice particle evolution under different conditions.

Acknowledgements. This research was supported by the National Natural Science Foundation of China (Grant No. 41175120) and the Knowledge Innovation Program of the Chinese Academy of Sciences (Grant No. KZCX2-EW-203).

REFERENCES

Baumgardner, D., 1983: An analysis and comparison of five water droplet measuring instruments. *J. Appl. Meteor.*, **22**, 891–910.

Baumgardner, D., and A. Korolev, 1997: Airspeed corrections for optical array probe sample volumes. *J. Atmos. Oceanic Technol.*, **14**, 1224–1229.

Biter, C. J., J. E. Dye, D. Huffman, and W. D. King, 1987: The drop-size response of the CSIRO liquid water probe. *J. Atmos. Oceanic Technol.*, **4**, 359–367.

Carey, L. D., J. G. Niu, P. Yang, J. A. Kankiewicz, V. E. Larson, and T. H. V. Haar, 2008: The vertical profile of liquid and ice water content in midlatitude mixed-phase altocumulus clouds.

J. Appl. Meteor. Climatol., **47**, 2487–2495.

Choi, Y.-S., C.-H. Ho, S.-W. Kim, and R. S. Lindzen, 2010: Observational diagnosis of cloud phase in the winter Antarctic atmosphere for parameterizations in climate models. *Adv. Atmos. Sci.*, **27**, 1233–1245, doi: 10.1007/s00376-010-9175-3.

Cober, S. G., J. W. Strapp, and G. A. Isaac, 1996: An example of supercooled drizzle drops formed through a collision-coalescence process. *J. Appl. Meteor.*, **35**, 2250–2260.

Cober, S. G., G. A. Isaac, and J. W. Strapp, 2001a: Characterizations of aircraft icing environments that include supercooled large drops. *J. Appl. Meteor.*, **40**, 1984–2002.

Cober, S. G., G. A. Isaac, A. V. Korolev, and J. W. Strapp, 2001b: Assessing cloud-phase conditions. *J. Appl. Meteor.*, **40**, 1967–1983.

Dye, J. E., and D. Baumgardner, 1984: Evaluation of the forward scattering spectrometer probe. Part I: Electronic and optical studies. *J. Atmos. Oceanic Technol.*, **1**, 329–344.

Fan, Y., X. L. Guo, D. G. Zhang, D. H. Fu, J. D. Chen, and Y. L. Ma, 2010: Airborne particle measuring system measurement on structure and size distribution of stratocumulus during August to September in 2004 over Beijing and its surrounding areas. *Chinese J. Atmos. Sci.*, **34**, 1187–1200. (in Chinese)

Field, P. R., 1999: Aircraft observations of ice crystal evolution in an altostratus cloud. *J. Atmos. Sci.*, **56**, 1925–1941.

Fowler, L. D., and D. A. Randall, 1996: Liquid and ice cloud microphysics in the CSU general circulation model. Part III: Sensitivity to modeling assumptions. *J. Climate*, **9**, 561–586.

Gardiner, B. A., and J. Hallett, 1985: Degradation of in-cloud forward scattering spectrometer probe measurements in the presence of ice particles. *J. Atmos. Oceanic Technol.*, **2**, 171–180.

Gordon, G. L., and J. D. Martwitz, 1986: Hydrometeor evolution in rainbands over the California valley. *J. Atmos. Sci.*, **43**, 1087–1100.

Hallett, J., and S. C. Mossop, 1974: Production of secondary ice particles during the riming process. *Nature*, **249**, 26–28.

Heymsfield, A. J., L. M. Miloshevich, A. Slingo, K. Sassen, and D. O. C. Starr, 1991: An observational and theoretical study of highly supercooled altocumulus. *J. Atmos. Sci.*, **48**, 923–945.

Hobbs, P. V., and A. L. Rangno, 1985: Ice particle concentrations in clouds. *J. Atmos. Sci.*, **42**, 2523–2549.

Hogan, R. J., P. N. Francis, H. Flentje, A. J. Illingworth, M. Quante, and J. Pelon, 2003: Characteristics of mixed-phase clouds. I: Lidar, radar and aircraft observations from CLARE'98. *Quart. J. Roy. Meteor. Soc.*, **129**, 2089–2116.

King, W. D., D. A. Parkin, and R. J. Handsworth, 1978: A hot-wire liquid water device having fully calculable response characteristics. *J. Appl. Meteor.*, **17**, 1809–1813.

Knollenberg, R. G., 1970: The optical array: An alternative to scattering or extinction for airborne particle size determination. *J. Appl. Meteor.*, **9**, 86–103.

Korolev, A. V., S. V. Kuznetsov, Y. E. Makarov, and V. S. Novikov, 1991: Evaluation of measurements of particle size and sample area from optical array probes. *J. Atmos. Oceanic Technol.*, **8**, 514–522.

Korolev, A. V., J. W. Strapp, and G. A. Isaac, 1998: Evaluation of the accuracy of PMS optical array probes. *J. Atmos. Oceanic Technol.*, **15**, 708–720.

Lawson, R. P., B. A. Baker, C. G. Schmitt, and T. L. Jensen, 2001: An overview of microphysical properties of Arctic clouds observed in May and July 1998 during FIRE ACE. *J. Geophys. Res.*, **106**, 14 989–15 014.

Lo, K. K., and R. E. Passarelli Jr., 1982: The growth of snow in winter storms: An airborne observational study. *J. Atmos. Sci.*, **39**, 697–706.

Mazin, I. P., 2006: Cloud phase structure: Experimental data analysis and parameterization. *J. Atmos. Sci.*, **63**, 667–681.

Niu, J. G., L. D. Carey, P. Yang, and T. H. Vonder Haar, 2008: Optical properties of a vertically inhomogeneous mid-latitude mid-level mixed-phase altocumulus in the infrared region. *Atmospheric Research*, **88**, 234–242.

Noh, Y.-J., C. J. Seaman, T. H. Vonder Haar, and G. S. Liu, 2013: In situ aircraft measurements of the vertical distribution of liquid and ice water content in midlatitude mixed-phase clouds. *J. Appl. Meteor. Climatol.*, **52**, 269–279.

Pinto, J. O., 1998: Autumnal mixed-phase cloudy boundary layers in the Arctic. *J. Atmos. Sci.*, **55**, 2016–2038.

Rotstayn, L. D., 1997: A physically based scheme for the treatment of stratiform clouds and precipitation in large-scale models. I: Description and evaluation of the microphysical processes. *Quart. J. Roy. Meteor. Soc.*, **123**, 1227–1282.

Shupe, M. D., S. Y. Matrosov, and T. Uttal, 2006: Arctic mixed-phase cloud properties derived from surface-based sensors at SHEBA. *J. Atmos. Sci.*, **63**, 697–711.

Strapp, J. W., F. Albers, A. Reuter, A. V. Korolev, U. Maixner, E. Rashke, and Z. Vukovic, 2001: Laboratory measurements of the response of a PMS OAP-2DC. *J. Atmos. Oceanic Technol.*, **18**, 1150–1170.

Sun, Z., and K. P. Shine, 1994: Studies of the radiative properties of ice and mixed-phase clouds. *Quart. J. Roy. Meteor. Soc.*, **120**, 111–137.

Ulbrich, C. W., 1983: Natural variations in the analytical form of the raindrop size distribution. *J. Climate Appl. Meteor.*, **22**, 1764–1775.

Williams, E. R., R. Zhang, and J. Rydock, 1991: Mixed-phase microphysics and cloud electrification. *J. Atmos. Sci.*, **48**, 2195–2203.

Wolde, M., and G. Vali, 2002: Cloud structure and crystal growth in nimbostratus. *Atmospheric Research*, **61**, 49–74.

Young, S. A., C. M. R. Platt, R. T. Austin, and G. R. Patterson, 2000: Optical properties and phase of some midlatitude, midlevel clouds in ECLIPS. *J. Appl. Meteor.*, **39**, 135–153.

Zhang, D. G., X. L. Guo, D. L. Gong, and Z. Y. Yao, 2011: The observational results of the clouds microphysical structure based on the data obtained by 23 sorties between 1989 and 2008 in Shandong Province. *Acta Meteorologica Sinica*, **69**, 195–207. (in Chinese)

Zhang, D. M., Z. Wang, and D. Liu, 2010: A global view of midlevel liquid-layer topped stratiform cloud distribution and phase partition from CALIPSO and CloudSat measurements. *J. Geophys. Res.*, **115**, doi: 10.1029/2009JD012143.

Zhong, L. Z., L. P. Liu, S. Feng, R. S. Ge, and Z. Zhang, 2011: A 35-GHz polarimetrie Doppler radar and its application for observing clouds associated with Typhoon Nuri. *Adv. Atmos. Sci.*, **28**, 945–956, 10.1007/s00376-010-0073-5.